

# RS model with a small curvature and two-photon production at the LHC

A.V. Kisselev\*

Institute for High Energy Physics, 142281 Protvino, Russia

## Abstract

The  $p_{\perp}$ -distribution for the diphoton production at the LHC is calculated in the modified Randall-Sundrum model with a small curvature of the space-time  $\kappa$ , and 5-dimensional Planck scale  $M_5$  in the TeV region. The discovery limits on  $M_5$  are obtained to be 9.4 TeV and 11.6 TeV for the integrated luminosities  $30 \text{ fb}^{-1}$  and  $100 \text{ fb}^{-1}$ , respectively. These limits do not depend on  $\kappa$  provided it is much smaller than  $M_5$ . The account of graviton widths is a crucial points of our calculations.

## 1 RS1 model with a small curvature

In this Section we will consider in details the Randall-Sundrum (RS) model with the small curvature. The main features and differences from a conventional (large curvature) scenario will be pointed to.

The RS model [1] is a theory with one extra dimension (ED) in a slice of the  $\text{AdS}_5$  space-time. It has the following background warped metric:

$$ds^2 = e^{2\kappa(\pi r_c - |y|)} \eta_{\mu\nu} dx^\mu dx^\nu + dy^2, \quad (1)$$

where  $y = r_c \theta$  ( $-\pi \leq \theta \leq \pi$ ),  $r_c$  being the “radius” of the ED, and  $\eta_{\mu\nu}$  is the Minkowski metric. The points  $(x_\mu, y)$  and  $(x_\mu, -y)$  are identified, so one gets the orbifold  $S^1/Z_2$ .

---

\*Electronic address: alexandre.kisselev@ihep.ru

The parameter  $\kappa$  defines a 5-dimensional scalar curvature of the AdS<sub>5</sub> space. For the sake of simplicity we will call  $\kappa$  “curvature”.

The so-called RS1 model has two 3D branes with equal and opposite tensions located at the points  $y = \pi r_c$  (called the TeV brane) and  $y = 0$  (referred to as the Planck brane). If  $k > 0$ , the tension on the TeV brane is negative, whereas the tension on the Planck brane is positive. All the SM fields are constrained to the TeV brane, while the gravity propagates in four spacial dimensions.

It is necessary to note that metric (1) is chosen in such a way that 4-dimensional coordinates  $x_\mu$  are Galilean on the TeV brane where all the SM field live, since the warp factor is equal to unity at  $y = \pi r_c$ .

By integrating 5-dimensional action over variable  $y$ , one gets an effective 4-dimensional action, that results in the “hierarchy relation” between the reduced Planck scale  $\bar{M}_{\text{Pl}}$  and 5-dimensional reduced gravity scale  $\bar{M}_5$ :

$$\bar{M}_{\text{Pl}}^2 = \frac{\bar{M}_5^3}{\kappa} (e^{2\pi\kappa r_c} - 1) . \quad (2)$$

The reduced gravity scale  $\bar{M}_5$  is related to the Planck mass  $M_5$  by the equation

$$M_5 = (2\pi)^{1/3} \bar{M}_5 \simeq 1.84 \bar{M}_5 . \quad (3)$$

Unless explicitly stated otherwise, we consider the *reduced* 5-dimensional Planck scale.

From the point of view of a 4-dimensional observer located on the TeV brane, there exists an infinite number of graviton KK excitations with the masses

$$m_n = x_n \kappa, \quad n = 1, 2 \dots , \quad (4)$$

where  $x_n$  are zeros of the Bessel function  $J_1(x)$ . Note that  $x_n \simeq \pi(n + 1/4)$ .

The interaction of the KK gravitons with the the SM fields on the TeV brane is described by the Lagrangian:

$$\mathcal{L}_{int} = -\frac{1}{\bar{M}_{\text{Pl}}} T^{\mu\nu} G_{\mu\nu}^{(0)} - \frac{1}{\Lambda_\pi} T^{\mu\nu} \sum_{n=1}^{\infty} G_{\mu\nu}^{(n)} . \quad (5)$$

Here  $T^{\mu\nu}$  is the energy-momentum tensor of the matter, and  $G_{\mu\nu}^{(n)}$  is the graviton field with the KK-number  $n$ . The parameter  $\Lambda_\pi$ ,

$$\Lambda_\pi = \bar{M}_5 \left( \frac{\bar{M}_5}{\kappa} \right)^{1/2} , \quad (6)$$

is the physical scale on the TeV brane.

Note that in most of the papers which treated the RS model (including Ref. [1]), the background metric was taken to be

$$ds^2 = e^{-2\kappa|y|} \eta_{\mu\nu} dx^\mu dx^\nu + dy^2, \quad (7)$$

instead of expression (1). In such a case, the hierarchy relation looks like

$$\bar{M}_{\text{Pl}}^2 = \frac{\bar{M}_5^3}{\kappa} (1 - e^{-2\pi\kappa r_c}), \quad (8)$$

with the graviton masses

$$m_n = x_n \kappa e^{-\pi\kappa r_c}, \quad n = 1, 2, \dots \quad (9)$$

In order the hierarchy relation (8) to be satisfied, while the lightest graviton masses to be around one TeV, one has to introduce two huge mass scales (*large curvature option*),

$$\kappa \sim \bar{M}_5 \sim \bar{M}_{\text{Pl}}, \quad (10)$$

and take  $\kappa r_c \simeq 12$ .

Thus, one obtains a series of graviton resonances with the lightest KK mode around one TeV. The experimental signature of the the RS model with the large curvature (10) is a real or virtual production of the massive KK graviton resonances.

There exists a serious shortcoming of the scenario with the curvature and fundamental gravity scale being of the order of the Planck mass (10). Namely, *kinetic terms* of the graviton fields on the TeV brane *do not have a canonical form*, and Lorentz indices are raised with the Minkowski tensor, while the metric in the coordinates  $x_\mu$  is  $e^{-\pi\kappa r} \eta_{\mu\nu}$  (for details, see Ref. [2]).

The correct interpretation of the effective 4-dimensional theory can be achieved by changing variables:

$$x^\mu \rightarrow z^\mu = x^\mu e^{-\pi\kappa r_c}. \quad (11)$$

As one can see, metric (7) turns into metric (1) under such a replacement.

In the present paper we will use an approach based on the metric (1) (*small curvature option* [3]-[5]) and put

$$\bar{M}_5 = (1 \div 20) \text{ TeV}, \quad \kappa = (0.1 \div 1) \text{ GeV}. \quad (12)$$

In order the hierarchy relation (2) to be satisfied, it is then necessary to take  $r_c\kappa \simeq 8 \div 9.5$ , i.e.  $r_c \simeq 0.15 \div 1.8$  fm. Thus, no large scales are introduced, contrary to the large curvature case. In what follows, the RS1 model with the small curvature will be referred to as *large warped dimension* scheme.

Instead of the fact that the size of the ED  $r_c$  is of the order of 1 fm, and masses of the first KK gravitons are relatively small, they give a negligible correction to the Newton law. Indeed, the Newton potential between two test masses  $m_1$  and  $m_2$  separated by the distance  $r$  is equal to

$$\begin{aligned} V(r) &= G_N \frac{m_1 m_2}{r} + \int_{m_1}^{\infty} \frac{dm}{\pi\kappa} G_N \frac{m_1 m_2}{r} e^{-mr} \\ &= G_N \frac{m_1 m_2}{r} \left( 1 + \frac{e^{-m_1 r}}{\pi\kappa r} \right). \end{aligned} \quad (13)$$

Since  $m_1 = x_1\kappa$ , where  $x_1 = 3.84$  is the first zero of the Bessel function  $J_1(x)$ , we find that the relative correction from the KK gravitons to the Newton law is less than  $2 \cdot 10^{-15}$ .

In our scheme, a coupling of the KK graviton with the SM fields is rather weak,<sup>1</sup> since

$$\Lambda_\pi = 100 \left( \frac{M_5}{\text{TeV}} \right)^{3/2} \left( \frac{100 \text{ MeV}}{\kappa} \right)^{1/2} \text{ TeV}. \quad (14)$$

However, in physical matrix elements the smallness of the coupling  $\Lambda_\pi^{-2}$  is compensated by the large number of real gravitons which can be produced or by infinite number of virtual gravitons. As a result, the matrix elements are defined by the 5-dimensional gravity scale  $\bar{M}_5$ , not by  $\Lambda_\pi$  or  $\kappa$  separately [4, 5]. This circumstance reminds that in the ADD model with flat EDs [8].

Previously, we studied gravity effects in the RS1 model with the small curvature in the scattering of ultrahigh neutrinos off the nucleon [4], in exclusive double diffractive events at the LHC [6], as well as in  $e^+e^-$  annihilation into lepton pairs at the ILC [7].

The goal of the present paper is to estimate gravity effects in a two-photon production at the LHC. The search limits on the fundamental Planck scale will be derived which are insensitive to the curvature of the warped space-time of the model.

---

<sup>1</sup>In the conventional scheme of the RS model,  $\Lambda_\pi \simeq 1$  TeV.

## 2 Virtual graviton contribution to a diphoton production

Diphoton final states are a signature of many interesting physics processes. For instance, one of the main discovery channels for the Higgs boson search at the LHC is the  $\gamma\gamma$  final state. An excess of  $\gamma\gamma$  production could be a signature of interactions beyond the SM. In addition, the diphoton final state is interesting in its own right. Using good energy resolution of the electromagnetic calorimeter [9], the transverse momentum of the photons,  $p_\perp$ , can be directly determined with a good precision. A possible excess in  $p_\perp$ -distribution could indicate effects coming from a new physics, in particular, from large EDs.

What is the reason to consider large warped dimension scenario? First, the spectrum of the KK gravitons (4) is very similar to that in the model with *one* ED [8] (see previous Section). Second, all matrix elements for the scattering of the SM fields can be formally obtained from corresponding matrix elements calculated in the model with one *flat* dimension by using the following replacement [4, 7]:

$$\bar{M}_{4+1} \rightarrow (2\pi)^{-1/3} \bar{M}_5, \quad R_c \rightarrow (\pi\kappa)^{-1}. \quad (15)$$

Here  $\bar{M}_{4+1}$  is a 5-dimensional reduced Planck scale,  $R_c$  being the radius of the extra flat dimension. As a result, all cross sections appear to be rather large (as in the ADD model with  $4+1$  dimensions). Finally, as was shown in Ref. [5], astrophysical restrictions are not applied to the RS model with the large ED (i.e. small graviton masses), if the curvature lies within the limits mentioned above (12).<sup>2</sup>

Let us consider the two-photon production with high transverse momenta ( $p_\perp \ll \sqrt{s}$  is assumed):

$$pp \rightarrow \gamma\gamma + X, \quad (16)$$

where  $X$  denotes a remnant of the colliding protons. The differential cross

---

<sup>2</sup>Actually, much smaller values of  $\kappa$  are allowed [5].

section is equal to

$$\begin{aligned} \frac{d\sigma}{dp_{\perp}^2}(pp \rightarrow \gamma\gamma + X) &= \sum_{a,b} \int_0^1 dx_a f_{a/p}(\mu^2, x_a) \int_0^1 dx_b f_{b/p}(\mu^2, x_b) \\ &\times \theta(x_a x_b - x_{\perp}^2) \frac{\sqrt{x_a x_b}}{\sqrt{x_a x_b - x_{\perp}^2}} \frac{d\hat{\sigma}}{d\hat{t}}(ab \rightarrow \gamma\gamma). \end{aligned} \quad (17)$$

Here  $f_{a/p}(\mu^2, x_a)$  is the distribution of the parton of the type  $a$  in momentum fraction  $x_a$  inside the proton taken at the factorization scale  $\mu$  (this scale will be fixed below).  $d\hat{\sigma}/d\hat{t}$  denotes the cross section of the hard sub-process  $ab \rightarrow \gamma\gamma$ . We have introduced the dimensional variable

$$x_{\perp} = \frac{2p_{\perp}}{\sqrt{s}}. \quad (18)$$

Throughout the paper,  $\hat{s}$ ,  $\hat{t}$  and  $\hat{u}$  denote Mandelstam variables of the *partonic sub-process* ( $\hat{s} + \hat{t} + \hat{u} = 0$ ,  $\hat{s} = s x_a x_b$ ,  $\hat{t}\hat{u}/\hat{s} = p_{\perp}^2$ ).

The contribution of the virtual gravitons to the process (16) comes from the quark-antiquark annihilation,

$$q \bar{q} \rightarrow G^{(n)} \rightarrow \gamma\gamma, \quad (19)$$

and gluon-gluon fusion,

$$g g \rightarrow G^{(n)} \rightarrow \gamma\gamma. \quad (20)$$

The matrix elements for both the partonic sub-processes (19)-(20) are given by the expression

$$\mathcal{M} = \mathcal{A} \mathcal{S}. \quad (21)$$

The first factor in the r.h.s. of Eq. (21) is

$$\mathcal{A} = T_{\mu\nu}^{q(g)} T^{\gamma\mu\nu} - \frac{1}{3} (T^{q(g)})_{\mu}^{\mu} (T^{\gamma})_{\nu}^{\nu}, \quad (22)$$

where  $T_{\mu\nu}^{q(g)}$  is the energy-momentum tensor of the quark (gluon) field,  $T_{\mu\nu}^{\gamma}$  is the photon energy-momentum tensor.

The graviton exchange in the  $s$ -channel leads to the following expression:

$$\mathcal{S}(\hat{s}) = \frac{1}{\Lambda_{\pi}^2} \sum_{n=1}^{\infty} \frac{1}{\hat{s} - m_n^2 + i m_n \Gamma_n}. \quad (23)$$

Here  $\Gamma_n$  denotes a total width of the graviton with the KK number  $n$  and mass  $m_n$ :

$$\Gamma_n = \eta m_n \left( \frac{m_n}{\Lambda_\pi} \right)^2, \quad (24)$$

with  $\eta \simeq 0.09$  [10]. The width is small provided  $n$  is not extremely large.

Then the relevant partonic cross sections are (see, for instance, formulae in Appendix of Ref. [3]):

$$\frac{d\hat{\sigma}}{d\hat{t}}(q\bar{q} \rightarrow \gamma\gamma) = \frac{\hat{t}^2 + \hat{u}^2}{192\pi\hat{s}^2\hat{t}\hat{u}} |2e_q^2 - \hat{t}\hat{u}\mathcal{S}(\hat{s})|^2, \quad (25)$$

$$\frac{d\hat{\sigma}}{d\hat{t}}(gg \rightarrow \gamma\gamma) = \frac{\hat{t}^4 + \hat{u}^4}{512\pi\hat{s}^2} |\mathcal{S}(\hat{s})|^2, \quad (26)$$

where  $e_q$  is the electric charge of the quark  $q$ .

In the region  $\sqrt{\hat{s}} \sim \bar{M}_5 \gg \kappa$ , the sum (23) can be calculated analytically, an explicit form of the function  $\mathcal{S}(\hat{s})$  was derived in Ref. [5]:

$$\mathcal{S}(\hat{s}) = -\frac{1}{4\bar{M}_5^3\sqrt{\hat{s}}} \frac{\sin 2A + i \sinh 2\varepsilon}{\cos^2 A + \sinh^2 \varepsilon}, \quad (27)$$

where

$$A = \frac{\sqrt{\hat{s}}}{\kappa}, \quad (28)$$

$$\varepsilon = \frac{\eta}{2} \left( \frac{\sqrt{\hat{s}}}{\bar{M}_5} \right)^3. \quad (29)$$

Should we ignore the widths of the massive gravitons, and replace the summation in KK number (23) by the integration in graviton masses using the relation  $dn = dm/(\pi\kappa)$ , we get

$$\text{Im } \mathcal{S}(\hat{s}) = -\frac{1}{2\bar{M}_5^3\sqrt{\hat{s}}}, \quad \text{Re } \mathcal{S}(\hat{s}) = 0, \quad (30)$$

in contrast to formula (27).

At  $\sqrt{\hat{s}} \gtrsim 3.5 \bar{M}_5$ , we get from (27)-(29):

$$\text{Im } \mathcal{S}(\hat{s}) \simeq -\frac{1}{2\bar{M}_5^3\sqrt{\hat{s}}}, \quad \text{Re } \mathcal{S}(\hat{s}) < 0.05 \text{Im } \mathcal{S}(\hat{s}). \quad (31)$$

The inequality  $\sqrt{\hat{s}} > 3.5 \bar{M}_5$  is equivalent to the inequality  $\Delta m_{KK} < \Gamma_n$ , where  $\Delta m_{KK}$  is the mass splitting, and  $\Gamma_n$  is the graviton width for relevant KK numbers (corresponding to  $m_n \sim \sqrt{\hat{s}}$ ) [5]. In such a case, one may regard a set of narrow graviton resonances to be a continuous mass spectrum.

However, the kinematical region for our treatment is  $\sqrt{\hat{s}} \leq \sqrt{s} < 3\bar{M}_5$ . In this case, expressions (30) become incorrect, and formula (27), which takes into account the *nonzero widths* of the KK gravitons, should be used.

In Appendix A we will demonstrate that our formula (27) is a correct expression for the function  $\mathcal{S}(s)$  (23).

### 3 5-dimensional Planck scale: LHC search limits

The main goal of this Section is to obtain the LHC search limit for the 5-dimensional Planck scale  $\bar{M}_5$ .

Recently, the RS1 model with the large extra dimension has been checked by the DELPHI Collaboration [11]. The gravity effects were searched for by studying photon energy spectrum in the process  $e^+e^- \rightarrow \gamma + \cancel{E}_\perp$ . No deviations from the SM prediction were seen. The limit on  $M_5$  obtained is 1.69 TeV at 95% CL [11]. It corresponds to the following bound on the *reduced* fundamental scale (see the relation between  $M_5$  and  $\bar{M}_5$  (3)):

$$\bar{M}_5 > 0.92 \text{ TeV} . \quad (32)$$

The search for large EDs (with flat metric) in the diphoton channel using of  $\approx 200 \text{ pb}^{-1}$  of data collected by the CDF and DØ experiments at  $\sqrt{s} = 1.96 \text{ TeV}$  (Run II) have been presented in Refs. [12]. The  $p_\perp$ -distribution up to  $\sim 200 \text{ GeV}$  has been measured. The data are in a good agreement with the SM background. DØ Collaboration has also performed the search for the massive gravitons (warped metric with the large curvature) in the diphoton channel using high integrated luminosity [13]. No evidence for resonant production of the gravitons has been found.

We should also mention the preliminary analysis by the CDF Collaboration based on  $1.2 \text{ fb}^{-1}$  of data [14]. No significant excess of the data over the expected background in  $\gamma\gamma + X$  events was observed in  $m(\gamma\gamma)$  and  $p_\perp$ -distribution.

In Figs. 1 we present the result of our calculations of gravity effects in the diphoton production  $p\bar{p} \rightarrow \gamma\gamma + X$  at the Tevatron. We used a set of



parton distribution functions (PDFs) from Ref. [15] based on an analysis of charged-leptons proton/deuteron data on deep inelastic scattering collected in the SLAC-CERN-HERA experiments.

Generally, *both* PDFs *and* differential cross sections in (17) should depend on the factorization scale  $\mu$  due to higher order corrections, that results in  $\mu$ -independent cross section of the diphoton production (16). We restrict ourselves by first order expressions for the partonic cross sections (25)-(26), and the factorization parameter is taken to be equal to the relevant mass scale  $\mu = \sqrt{\hat{s}}$ . A possible  $\mu$ -dependence will be analyzed below (see our comments after Eq. (36)).

Let  $N_S$  be a number of signal events,  $N_B$  - number of background events. We define the statistical significance  $\mathbb{S} = N_S/\sqrt{N_B}$ , and require a  $5\sigma$  effect. Then we obtain the following bound from the Tevatron data<sup>3</sup> (with the integrated luminosity  $\mathcal{L} = 1 \text{ fb}^{-1}$ ):

$$\bar{M}_5 > 0.81 \text{ TeV} . \quad (33)$$

In calculating numbers of events, we used a K-factor 1.5 for the SM background, while a conservative value of K=1 was taken for the signal.

Let us stress that in our approach, the limit on  $\bar{M}_5$  does not depend on the value of the parameter  $\kappa$ , provided the inequality  $\kappa \ll \sqrt{s}$  is satisfied (see Section 4 for details).

We expect that the gravity effects related with the virtual gluon exchange will be more significant at the LHC, since

$$\frac{d\sigma(\text{SM})}{dp_\perp} = \frac{1}{s^{3/2}} f(x_\perp, \ln s) , \quad (34)$$

where  $f(x_\perp, \ln s)$  depends weakly on  $s$  via scaling violation in PDFs. The gravity term  $d\sigma(\text{grav})/dp_\perp$  depends rather slowly on  $s$  (see Eq. (45)). Thus, we obtain:

$$\frac{d\sigma(\text{grav})}{d\sigma(\text{SM})} \sim \left( \frac{\sqrt{s}}{\bar{M}_5} \right)^3 . \quad (35)$$

Correspondingly, the search limit for the LHC can be roughly estimated to be  $\bar{M}_5 = (6 \div 7) \text{ TeV}$ .

In order to obtain a correct search limit for the LHC, we have calculated contributions of  $s$ -channel gravitons to  $p_\perp$ -distributions of the final photons

---

<sup>3</sup>Let us notice, this bound is not the main goal of the paper.

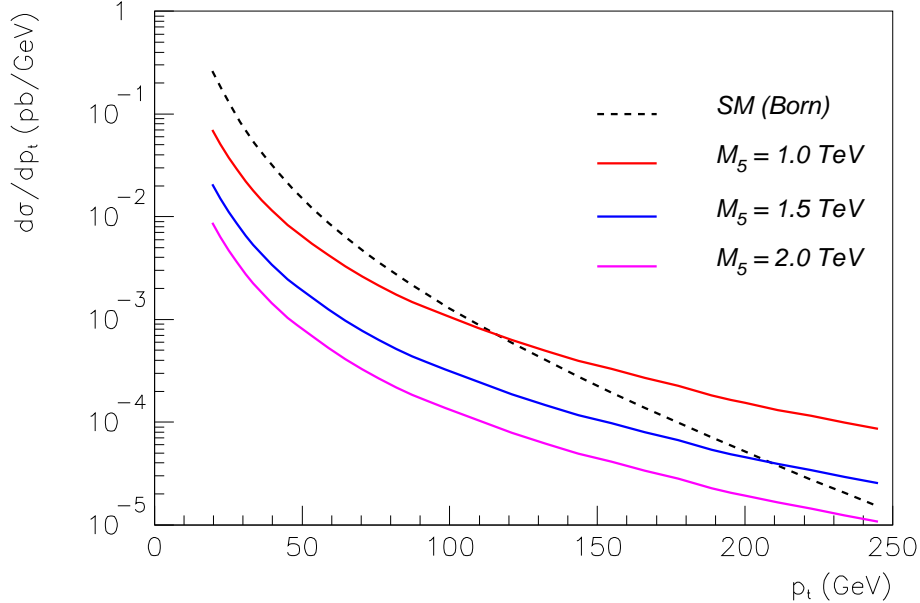


Figure 1: The graviton contributions (including the interference term) to the process  $p\bar{p} \rightarrow \gamma\gamma + X$  (solid curves) vs. SM contribution (dashed curve) at the Tevatron. In this and all subsequent figures,  $M_5$  denotes the *reduced* fundamental Planck mass.

for different values of  $\bar{M}_5$  (see Fig. 2). The ratio of the gravity induced term to the SM one is presented on the next plot (see Fig. 3). The ratio rises monotonically with  $p_\perp$  for all  $\bar{M}_5$ . Its dependence on  $\bar{M}_5$  is in accordance with Eq. (35). The details of our calculations are discussed in Section 4.

Taking into accounts the K-factors described above, we obtain histograms in Fig. 4 which show a number of events per 35 GeV bin at the integrated luminosity  $\mathcal{L} = 1 \text{ fb}^{-1}$ . A statistical significance as a function of the 5-dimensional Planck scale is presented in Fig. 5. Thus, we obtain the discovery limit of the LHC in the two-photon production in the RS1 model with the small curvature:

$$\bar{M}_5 = \begin{cases} 6.3 \text{ TeV} , & \mathcal{L} = 100 \text{ fb}^{-1} \\ 5.1 \text{ TeV} , & \mathcal{L} = 30 \text{ fb}^{-1} \end{cases} \quad (36)$$

Let us stress that this limit (36) do not depend on the ratio  $\kappa/\bar{M}_5$ , contrary to the conventional RS scenario (7) in which both the curvature  $\kappa$  and  $\bar{M}_5$  are of order of the 4-dimensional Planck mass (10).

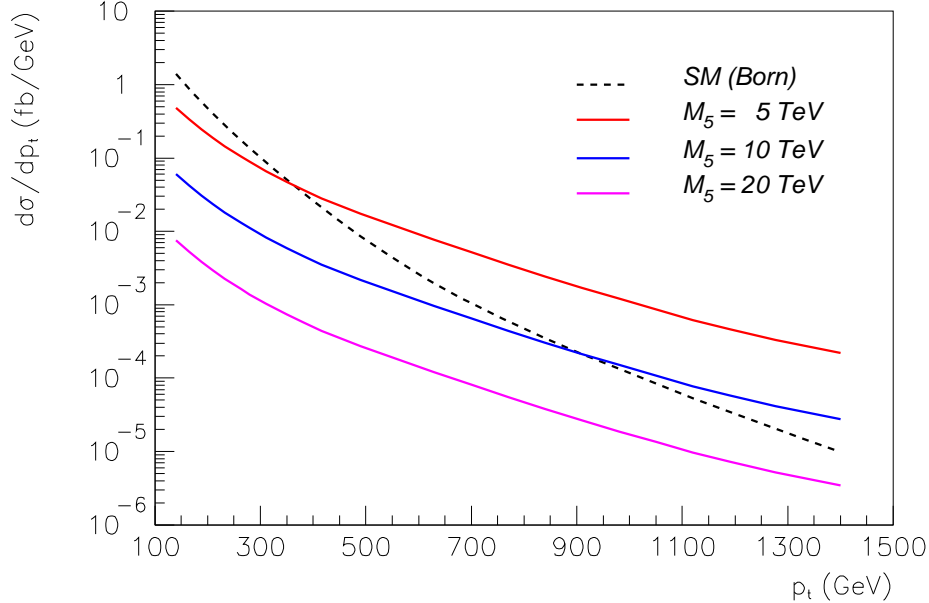


Figure 2: The s-channel graviton contribution to the process  $pp \rightarrow \gamma\gamma + X$  for different values of  $\bar{M}_5$  (solid curves) vs. SM contribution (dashed curve) at the LHC.

In order to estimate systematic theoretical uncertainties, we have calculated  $p_\perp$ -distributions for different values of the PDF scale  $\mu$ :  $\mu^2 = \hat{s}$ ,  $\mu^2 = 2\hat{s}$ , and  $\mu^2 = \hat{s}/2$ . It has appeared that an uncertainty in  $d\sigma(\text{grav})$  related with the PDF scale varies from 1.3% at  $p_\perp = 140$  GeV to 6.4% at  $p_\perp = 1$  TeV.<sup>4</sup> As for uncertainty in the ratio  $d\sigma(\text{grav})/d\sigma(\text{SM})$ , it decreases slowly from 2.8% to 2.1%, respectively.<sup>5</sup> As a result, the systematic uncertainty for  $\bar{M}_5$  from the PDF scale amounts to  $\Delta\bar{M}_5 = 17$  GeV at  $\mathcal{L} = 30 \text{ fb}^{-1}$ . Another systematic theoretical error comes from an uncertainty in cross sections due to a certain proton PDFs. Adopting that it does not exceed 2.7% [15], we get  $\Delta\bar{M}_5 = 23$  GeV.

One of systematic experimental uncertainties contributing to the number of events comes from luminosity measurements. The design precision of the luminosity is 5% at  $\mathcal{L} = 1 \text{ fb}^{-1}$  [9]. However, for measurements based on

<sup>4</sup>Note, it is lower values of  $p_\perp$  that are actually relevant for a calculation of the significance  $\mathbb{S}$ .

<sup>5</sup>All these numbers are *insensitive* to the value of  $\bar{M}_5$ .

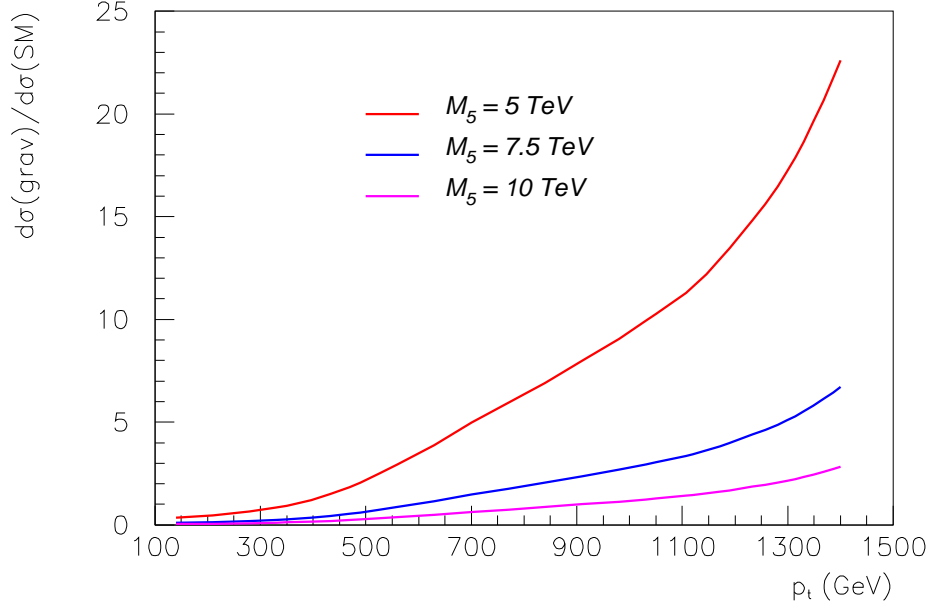


Figure 3: The ratio of the gravity induced cross section to the SM cross section for the diphoton production at the LHC as a function of the photon transverse momentum.

$\mathcal{L} = 30 \text{ fb}^{-1}$  or more, it is assumed that a 3% uncertainty can be achieved [9] that results in  $\Delta\bar{M}_5 = 26 \text{ GeV}$ . The error in measurements of the photon transverse momenta is less than 0.74% at  $p_\perp \geq 140 \text{ GeV}$  [9].

Rather small values of  $\Delta\bar{M}_5$  cited above may be understood as follows. Consider, for instance, the case when  $N_S$  and  $N_B$  increased by the factor  $(1 + \rho)$  due to an increase of the integrated luminosity ( $\rho \ll 1$ ). Then a corresponding variation of the significance  $\mathbb{S}$  can be compensated by much smaller variation of the 5-dimensional gravity scale:  $\bar{M}_5 \rightarrow \bar{M}_5 + \Delta\bar{M}_5 \simeq \bar{M}_5 (1 + \rho/6)$ .

Finally, let us demonstrate that an ignorance of the graviton widths would be a *very rough approximation*. Fig. 6 shows the gravity contribution to the  $p_\perp$ -distribution calculated with the use of equations (30). The significant difference of Fig. 6 from Fig. 2 can be explained as follows. As one can see from Appendix A, after integrating over  $s$ ,  $\text{Re } \mathcal{S}(s)$  averages to 0, while  $\text{Im } \mathcal{S}(s)$  averages approximately to 1. However, the expressions for the partonic cross sections (25), (26), contain quadratic term  $|\mathcal{S}(s)|^2$  as well as  $s$ -dependent

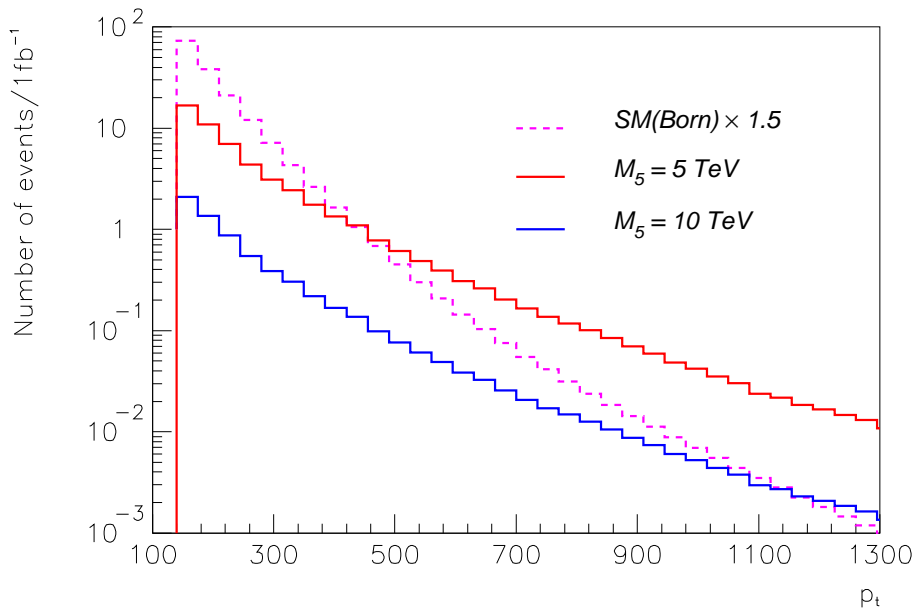


Figure 4: The expected number of events per 35 GeV bin at the integrated luminosity  $\mathcal{L} = 1 \text{ fb}^{-1}$  for the diphoton production at the LHC. The solid histograms denote the gravity contributions, while the dashed one corresponds to the SM (Born) term times K-factor 1.5.

factors. Moreover, the region of integration over parton momentum fractions  $x_a, x_b$  (see Eq. (17)) depends on  $s$ , since  $x_a x_b \geq 4p_{\perp}^2/s$ .

Thus we conclude that the account of the width of the KK gravitons is a crucial point for obtaining a correct result.

## 4 Important features and details of calculations

In this Section, we will discuss some details of calculations of the  $p_{\perp}$ -distribution for the diphoton production at the LHC, and analyze a possible dependence of this distribution on the parameters  $\bar{M}_5$  and  $\kappa$ . In particular, we will show that actually the distribution does not depend on  $\kappa$  (or, equivalently, on the ratio  $\kappa/\bar{M}_5$ , which is taken to be small, see Eq. (12)).

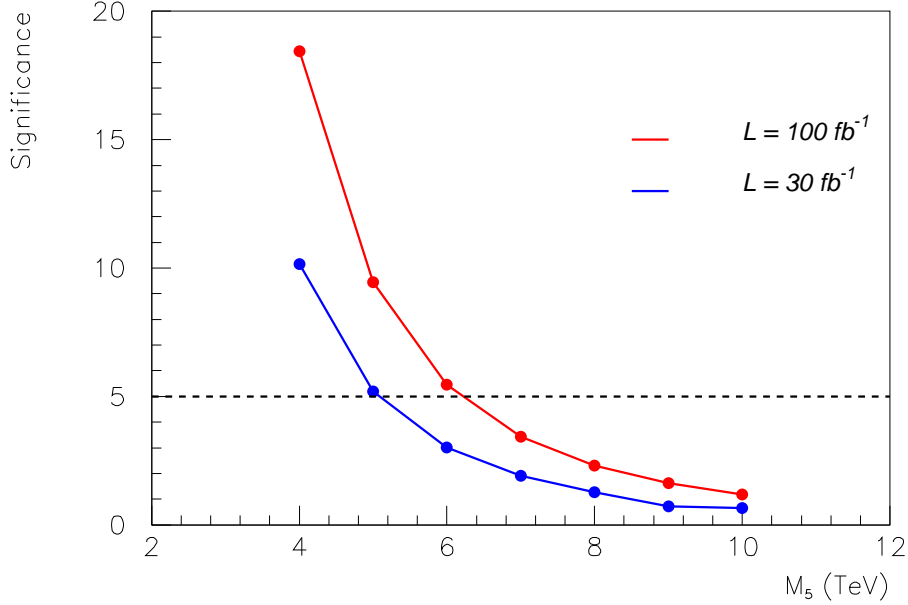


Figure 5: The statistical significance for the process  $pp \rightarrow \gamma\gamma + X$  at the LHC as a function of the 5-dimensional (reduced) Planck scale.

We start from formula (17). After changing variables,

$$x = x_a, \quad \tau = x_a x_b, \quad (37)$$

it has the following form:

$$\begin{aligned} \frac{d\sigma}{dp_{\perp}^2}(pp \rightarrow \gamma\gamma + X) &= \sum_{a,b} \int_{x_{\perp}^2}^1 \frac{d\tau \sqrt{\tau}}{\sqrt{\tau - x_{\perp}^2}} \int_{\tau}^1 \frac{dx}{x} f_{a/p}(\mu^2, x) f_{b/p}(\mu^2, \tau/x) \\ &\times \frac{d\hat{\sigma}}{d\hat{t}}(ab \rightarrow \gamma\gamma), \end{aligned} \quad (38)$$

where the partonic cross section  $d\hat{\sigma}/d\hat{t}$  depends on the function  $\mathcal{S}(\hat{s})$  (27). Since  $\hat{s} = s\tau$ , the latter is a function of  $\tau$ . It is convenient to define

$$\tilde{\mathcal{S}}(\tau) = [-4\bar{M}_5^3 \sqrt{s\tau}] \mathcal{S}(\tau). \quad (39)$$

Let  $A = A_0 + a$ , where  $A_0 = (n_0 + 1/2)\pi$ ,  $n_0$  being an integer, and  $|a| \ll 1$ . In a small vicinity of the point  $\tau_0 = (A_0 \kappa / \sqrt{s})$ , the function  $\tilde{\mathcal{S}}(\tau)$  can be well

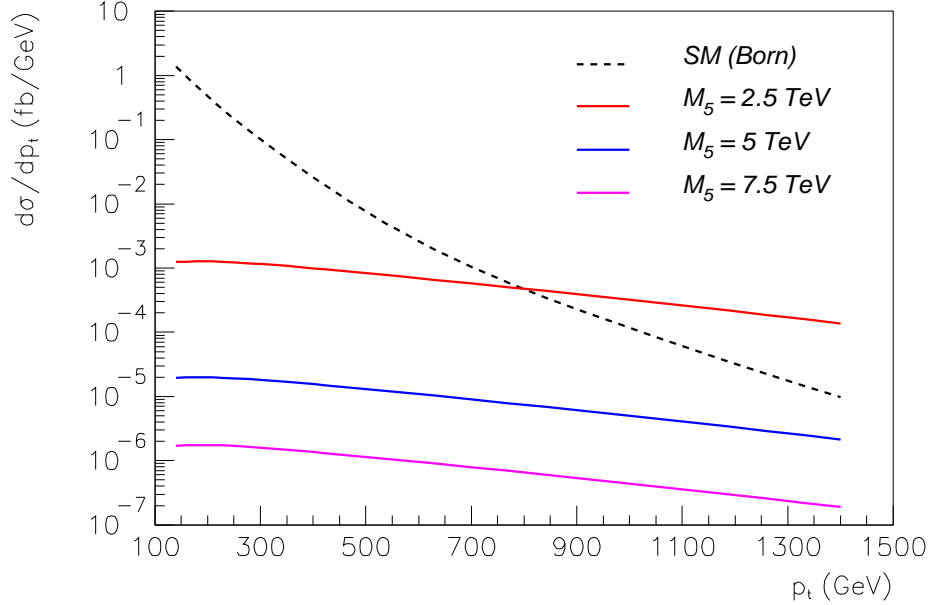


Figure 6: The same as in Fig. 2 (except for values of  $\bar{M}_5$ ), but calculations were done for *zero widths* of the KK gravitons (see formulae (30)).

approximated by the expression

$$\tilde{\mathcal{S}}(\tau) \simeq -\frac{2a - 2i\varepsilon_0}{a^2 + \varepsilon_0^2}, \quad (40)$$

where

$$\varepsilon_0 = \frac{\eta}{2} \left( \frac{\sqrt{s}\tau_0}{\bar{M}_5} \right)^3. \quad (41)$$

We have taken into account that  $\varepsilon_0 \ll 1$  for the relevant values of  $\sqrt{s}$  and  $\bar{M}_5$  (i.e. for  $\sqrt{s} = 14$  TeV,  $\bar{M}_5 \gtrsim 5$  TeV).

One can see from (40) that the real part,  $\text{Re}\tilde{\mathcal{S}}(\tau)$ , equals zero at  $\tau = \tau_0$  and has two extremal points at  $\tau = \tau_0 \pm \delta$ , where<sup>6</sup>

$$\delta = \eta\tau_0^2 \frac{\kappa s}{\bar{M}_5^3}. \quad (42)$$

As for the imaginary part,  $\text{Im}\tilde{\mathcal{S}}(\tau)$ , it has a very sharp peak at  $\tau = \tau_0$ . Two

<sup>6</sup>The relation  $\tau = \tau_0 \pm \delta$  is equivalent to the relation  $a = \pm \varepsilon_0$ .

peaks in the real part of the resonance are separated by the distance  $2\delta$ , the width of the imaginary of the resonance is also equal to  $\Gamma_S = 2\delta$ .

The forms of the real and imaginary parts of  $\tilde{\mathcal{S}}(\tau)$  are presented in Fig. 7 and Fig. 8, with  $\Delta\tau = 10\delta$  on both the figures. All the curves were calculated using the values of  $\bar{M}_5 = 20$  TeV,  $\kappa = 1$  GeV.

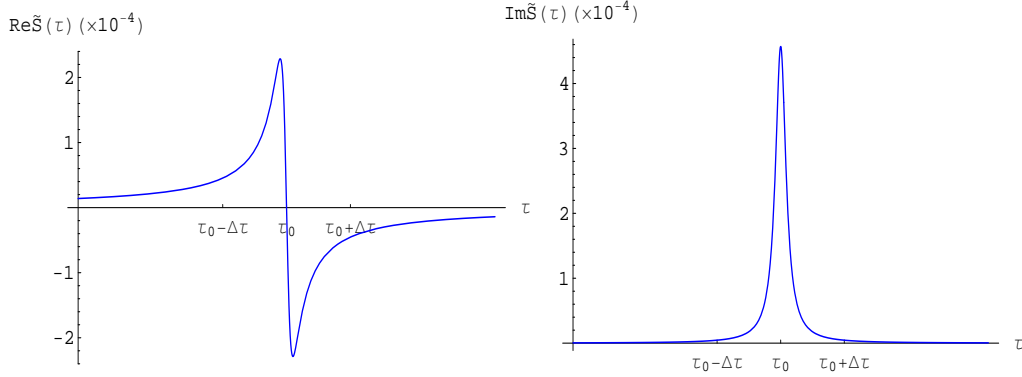


Figure 7: The real and imaginary parts of one of the resonances in the function  $\tilde{\mathcal{S}}(\tau)$  which describes virtual graviton contributions to partonic sub-processes. Both the curves correspond to  $\tau_0 = 0.02$ ,  $\Delta\tau = 8.8 \cdot 10^{-9}$ .

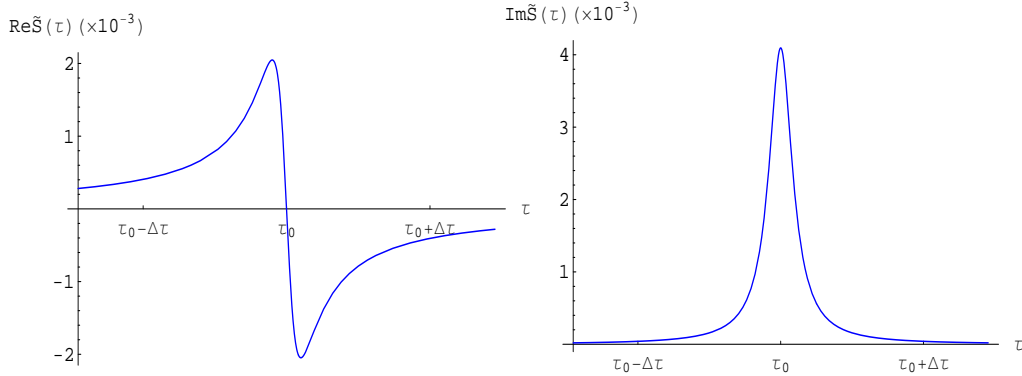


Figure 8: The same as in Figs. 7, but for another peak in  $\tilde{\mathcal{S}}(\tau)$  located at  $\tau_0 = 0.1$ , with  $\Delta\tau = 2.2 \cdot 10^{-7}$ .

Let us describe Fig. 7 first. The value of  $\tau_0 = 0.02002$  was taken, that corresponds to the equation  $\sqrt{s\tau_0}/\kappa = (630 + 1/2)\pi$ . Than we obtain that  $\Gamma_S \simeq 1.8 \cdot 10^{-9}$ . The calculations show that the next resonance is located



at the point  $\tau_0 = 0.02008$ . Thus, an average distance between neighboring peaks is much larger than their widths. It reflects the fact that one cannot regard a set of narrow resonances to be a continuous spectrum [5].

In the next two plots (see Fig. 8),  $\tau_0 = 0.10004$ ,  $n_0 = 1409$ , and  $\Gamma_S \simeq 4.4 \cdot 10^{-8}$ . A neighboring resonance with the number  $n_0 = 1410$  is located at  $\tau_0 = 0.10018$ .

The differential cross section of the process under consideration is represented in the form:

$$d\sigma = d\sigma(\text{SM}) + d\sigma(\text{grav}) + d\sigma(\text{SM-grav}) , \quad (43)$$

where the last term comes from the interference between the SM and graviton interactions. Since the SM amplitude is pure real, while the real part of each graviton resonance is antisymmetric with respect to its central point  $\tau_0$  (see the first curves in Figs. 7-8), the interference term in (43) has appeared to be negligible in comparison with the pure gravity contribution (the second term in (43)) after integration in variable  $\tau$ .

The smaller is the value of  $\tau_0$ , the narrower is the peak and larger is its height (compare, for instance, the curves in Fig. 7 and Fig. 8). The latter circumstance means that only a smaller part of the graviton resonances is significant for numerical calculations. The total number of the graviton resonances which contribute to the differential cross section is equal to  $N = \text{Int}[\sqrt{s}(1 - x_\perp)/(\kappa\pi)]$ , with  $\text{Int}[z]$  being an integer part of  $z$ .<sup>7</sup> Actually, the main contribution to  $d\sigma(\text{grav})$  comes from, approximately,  $(1/7)N$  first resonances, while the account of the rest of  $(6/7)N$  resonances results in a few percent correction.

From all said above, we find that the gravity contribution to the partonic cross section is proportional to

$$s^2 \left[ \frac{1}{\bar{M}_5^3 \sqrt{s} \varepsilon_0} \right]^2 \delta N \sim \frac{1}{\bar{M}_5^3 \sqrt{s}} . \quad (44)$$

In other words, we obtain that the differential cross section (38) *does not depend on the curvature*, and

$$\frac{d\sigma(\text{grav})}{dp_\perp} = \frac{1}{\bar{M}_5^3} F(x_\perp, \ln s) , \quad (45)$$

---

<sup>7</sup>The variable  $x_\perp$  was defined above (18).

A weak  $s$ -dependence of  $F(x_\perp, \ln s)$  comes from the PDF scale. The numerical calculations *do confirm* that the differential cross section of the process (16) does not depend on  $\kappa$  and decreases as the third power of the fundamental gravity scale  $\bar{M}_5$ .

At small values of  $x_\perp$ , the main contribution to the  $p_\perp$ -distribution comes from the gluon-gluon fusion (20). Assuming that  $g(\mu^2, x) \sim x^{-1}$ , we get a *rough* estimate from (38):

$$\frac{d\sigma(\text{grav})}{dp_\perp} \sim x_\perp \int_{x_\perp^2}^1 d\tau \frac{1}{\tau^{5/2} \sqrt{\tau - x_\perp^2}} \ln \frac{1}{\tau} \sim \frac{1}{p_\perp^3} \ln \frac{1}{p_\perp}. \quad (46)$$

This form of  $d\sigma(\text{grav})/dp_\perp$  is in satisfactory agreement with our numerical calculations at  $p_\perp \ll \sqrt{s}$  (see Figs. 1, 2).

In order to get a correct numerical result, we divided a region of integration in variable  $\tau$  into small subregions around the resonance peaks. Since a typical value of  $N/7$  exceeds 600 ( $N = 4367$  for  $x_\perp = 0.02$ ,  $\kappa = 1$  GeV), it took lots of computer time. Fortunately, a number of integrations could be reduced if we use the facts that the gravity cross section is actually independent of  $\kappa$ , while  $N \sim \kappa^{-1}$ .

## 5 Conclusions

In the present paper the model with one large warped extra dimension (i.e. the RS1 scheme with the small curvature  $\kappa$ ) is studied [4, 5]. In such an approach, the reduced fundamental gravity scale  $\bar{M}_5$  lies in the TeV region (i.e. varies from one to tens TeV), and  $\kappa \ll \bar{M}_5$ . The mass spectrum is similar to that in the ADD model [8] with one flat extra dimension.

We have calculated the  $p_\perp$ -distribution for the process  $pp \rightarrow \gamma\gamma + X$  at the LHC, with  $p_\perp$  being the transverse momenta of the final photons. The LHC discovery limit on the reduced fundamental gravity scale  $\bar{M}_5$  has been obtained which is given by Eq. (36). Remembering relation between the 5-dimensional Planck mass  $M_5$  and its reduced value  $\bar{M}_5$  (3), we find the reach of the LHC in the search for the RS gravitons decaying into diphoton channel:

$$M_5 = \begin{cases} 11.6 \text{ TeV}, & \mathcal{L} = 100 \text{ fb}^{-1} \\ 9.4 \text{ TeV}, & \mathcal{L} = 30 \text{ fb}^{-1} \end{cases} \quad (47)$$

In the conventional RS scenario [1], both  $\kappa$  and  $\bar{M}_5$  are of order of the 4-dimensional Planck mass,  $\kappa \sim \bar{M}_5 \sim M_{\text{Pl}}$ . A search limit on the lightest graviton mass depends crucially on the ratio  $\kappa/\bar{M}_5$ . On the contrary, our bounds (47) do not depend on  $\kappa$ , since the gravity cross sections are insensitive to its value (provided  $\kappa \ll M_5$ ).

We have shown that neglecting the width of the KK gravitons would give us incorrect results. A zero width approximation is valid only if an effective collision energy of partonic sub-processes is at least 3.5 times larger than  $\bar{M}_5$  (see Eq. (31)).

## Acknowledgements

I am grateful to V.A. Petrov for fruitful discussions and critical remarks.

## References

- [1] L. Randall and R. Sundrum, Phys. Rev. Lett. **83**, 3370 (1999).
- [2] E.E. Boos, Yu.A. Kubyshin,, M.N. Smolyakov and I.P. Volobuev, Class. Quan. Grav. **19**, 4591 (2002); E.E. Boos, Yu.S. Mikhailov, M.N. Smolyakov and I.P. Volobuev, Nucl. Phys. B **717**, 19 (2005).
- [3] G.F. Giudice, T. Plehn and A. Strumia, Nucl. Phys. B **706**, 455 (2005).
- [4] A.V. Kisselev and V.A. Petrov, Phys. Rev. D **71**, 124032 (2005).
- [5] A.V. Kisselev, Phys. Rev. D **73**, 024007 (2006). .
- [6] A.V. Kisselev, V.A. Petrov and R.A. Ryutin, Phys. Lett.B **630**, 100 (2005).
- [7] A.V. Kisselev, JHEP 03, 006 (2007)
- [8] N. Arkani-Hamed, S. Dimopoulos and G. Dvali, Phys. Lett. B **429**, 263 (1998); I. Antoniadis, N. Arkani-Hamed, S. Dimopoulos and G. Dvali, Phys. Lett. B **436**, 257 (1998); N. Arkani-Hamed, S. Dimopoulos and G. Dvali, Phys. Rev. D **59**, 086004 (1999).

- [9] CMS Collaboration 2006 Technical Design Report, Volume I, CERN/LHCC 2006-001, CMS TDR 8.1; CMS Collaboration 2007 Technical Design Report, Volume II: Physics Performance, J. Phys. G: Nucl. Part.Phys. **34**, 995 (2007).
- [10] A.V. Kisselev, Eur. Phys. J. C **42**, 217 (2005).
- [11] K. Klein, Proceeding of the 34th International Conference on High Energy Physics (ICHEP 2006), July 26 - August 2, 2006, Moscow, Russia, p. 1133; S. Ask, V. Hedberg and F.-L. Navarria, Contributed paper for the 23rd International Symposium on Lepton-Photon Interactions at High Energy (LP07), August 13-18, 2007, Daegu, Korea.
- [12] B. Abbott *et al.*, (DØ Collaboration), Phys Rev. Lett. **86**, 1156 (2001); DØ Note 4336-Conf (2004); D. Acosta *et al.* (CDF Collaboration), Phys Rev. Lett. **95**, 022003 (2005).
- [13] V.M. Abazov *et al.*, (DØ Collaboration), Phys Rev. Lett. **95**, 091801 (2005); Phys Rev. Lett., accepted for publication (arXiv:07103338 (2007)).
- [14] A. Pronko, Proceeding of the 34th International Conference on High Energy Physics (ICHEP 2006), July 26 - August 2, 2006, Moscow, Russia, p. 1163.
- [15] S.I. Alekhin, JETP Lett. **82**, 628 (2005).

## Appendix A

In this Appendix we will present a result of computations of the function  $\mathcal{S}(s)$  with the use of three different equations (27), (30), and (23).

Let us define the dimensionless function:

$$\bar{\mathcal{S}}(s) = [-2\bar{M}_5^3\sqrt{s}] \mathcal{S}(s) . \tag{A.1}$$

The real and imaginary parts of  $\bar{\mathcal{S}}(s)$  in the energy region around the point  $\sqrt{s_0} = 5$  TeV are shown in Fig. 9 and Fig. 10, respectively. The values of the parameters were chosen to be  $\bar{M}_5 = 5$  TeV,  $\kappa = 1$  GeV. The resonance structures on both figures are obtained by using formula (27), while the solid

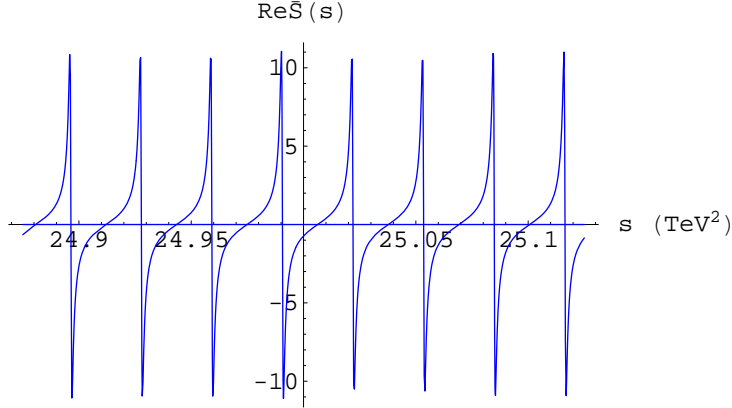


Figure 9: The real part of  $\bar{\mathcal{S}}(s)$  calculated by using Eq. (27). The line  $\text{Re}\bar{\mathcal{S}}(s) = 0$  corresponds to Eq. (30). The values of the parameters are:  $\bar{M}_5 = 5$  TeV,  $\kappa = 1$  GeV.

lines correspond to “zero width” equation (30). One can see that formula (30) is incorrect.

To demonstrate that our formula (27) is a correct expression for  $\mathcal{S}(s)$ , one should calculate the sum (23). It appeared that only the terms closed to  $n = n_0$ , where  $m_{n_0} = x_{n_0}\kappa \simeq \sqrt{s_0}$ , are important in the sum. For a sake of simplicity, we consider only the imaginary part of  $\bar{\mathcal{S}}(s)$ . In Fig. 11 we present the function  $\ln \text{Im}\bar{\mathcal{S}}(s)$  calculated for the case when only two terms in the sum, namely,  $n = n_0$  and  $n = n_0 + 1$ , are taken into account. The curve in the next figure corresponds to the case when already eight neighboring terms are taken into account.<sup>8</sup>

A comparison of Fig. 12 with Fig. 10 demonstrates us that our formula (27) is a nice approximation of the original expression (23).

---

<sup>8</sup>For a wider region of  $s$  more terms have to be considered in the sum (23).

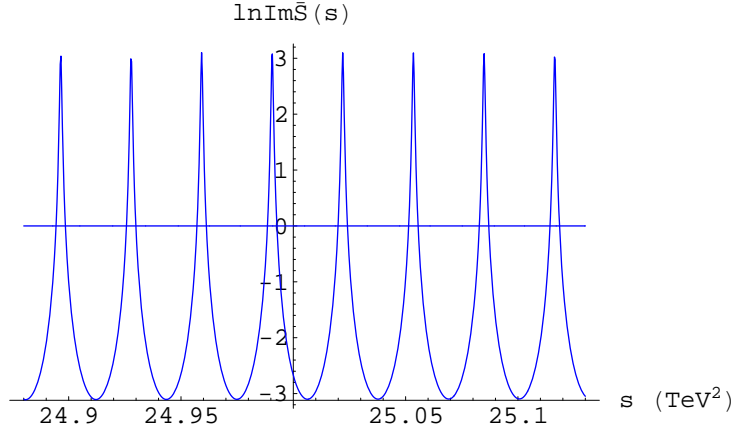


Figure 10: The function  $\ln \text{Im} \bar{\mathcal{S}}(s)$  calculated by using Eq. (27). The horizontal line corresponds to  $\text{Im} \bar{\mathcal{S}}(s) = 1$  (see Eq. (30)). The values of the parameters are the same as in Fig. 9.

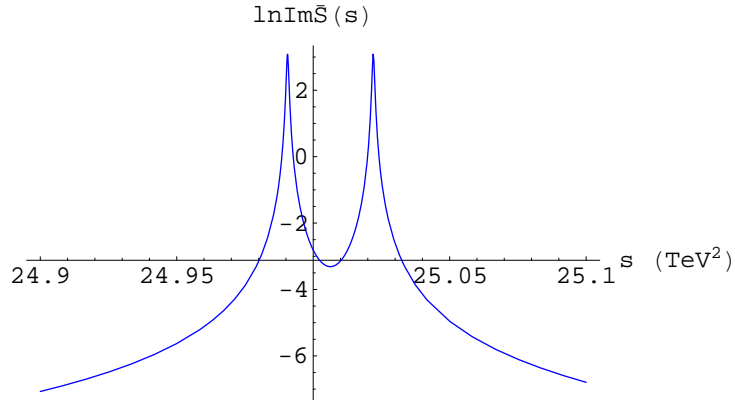


Figure 11: The imaginary part of  $\bar{\mathcal{S}}(s)$  calculated by using Eq. (23). Only two terms in the sum are taken into account. The values of the parameters are the same as in Fig. 10.

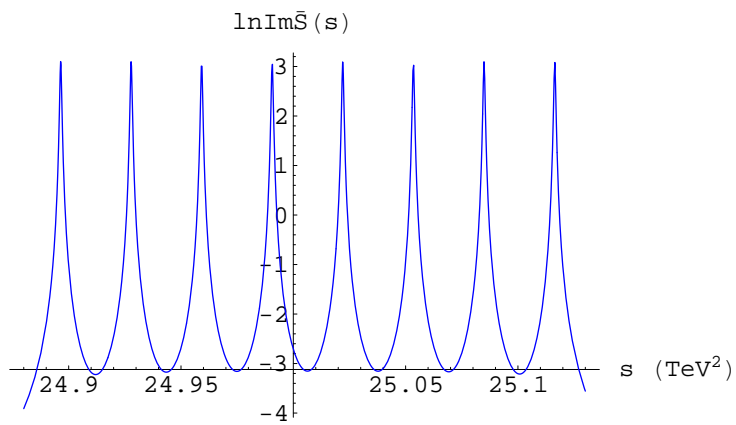


Figure 12: The same as in Fig. 11 but with eight terms taken into account in Eq. (23).